Ore Geology Reviews 36 (2009) 221–234

Contents lists available at ScienceDirect

Ore Geology Reviews

journal homepage: www.elsevier.com/locate/oregeorev

Geological and geochemical constraints on the origin of the giant Lincang coal seam-hosted germanium deposit, Yunnan, SW China: A review

Rui-Zhong Hu [a,*], Hua-Wen Qi [a], Mei-Fu Zhou [b], Wen-Chao Su [a], Xian-Wu Bi [a], Jian-Tang Peng [a], Hong Zhong [a]

[a] The State Key Laboratory of Ore Deposit Geochemistry, Institute of Geochemistry, Chinese Academy of Sciences, Guiyang, China
[b] Department of Earth Sciences, The University of Hong Kong, Hong Kong, China

ARTICLE INFO

Article history:
Received 24 October 2007
Received in revised form 25 February 2009
Accepted 25 February 2009
Available online 11 March 2009

Keywords:
Germanium
Coal
Siliceous rock
Hydrothermal fluids
Lincang germanium deposit
SW China

ABSTRACT

The Lincang germanium deposit, Yunnan, SW China, contains at least 1000 tonnes of Ge at an average grade of ~850 ppm Ge, and is one of the largest Ge deposits in the world. The deposit is hosted within coal seams of the Miocene Bangmai Formation, deposited on top of a Ge-rich granite batholith. The Bangmai Formation is divided into eight units among which three are coal-bearing. The Ge-bearing coal seams are inter-layered with siliceous rocks and siliceous limestones in the basal coal-bearing unit. The coal seams of the other two coal-bearing units are not interbedded with siliceous rocks and siliceous limestones, and are also barren with respect to Ge. Equant or elongate Ge-orebodies are generally located at fault intersections. Germanium is mainly associated with organic matter within the coal seams and is concentrated at the top and bottom of the coal seams, where the latter are in contact with the layered siliceous rocks or siliceous limestones. Major and trace element contents, and O- and C-isotopes of the siliceous rocks and siliceous limestones, are similar to those of hydrothermal sediments, indicating formation by hydrothermal sedimentation. Compared with barren coals, Ge-rich coals are notably rich in Nb, Li, Sb, W, Bi and U and show substantial enrichment of HREE which increase together with Ge. Germanium-rich coals contain disseminated pyrite with $\delta^{34}S$ ranging from 17.2 to 51.4‰, similar to pyrite in barren coals, and thin vein-like pyrite with $\delta^{34}S$ ranging from −5.4 to 1.9‰, similar to sulfides in granite-related quartz veins. We propose that circulating hydrothermal fluids leached abundant Ge and other elements from Ge-rich granites in the basement, and were then discharged into the basin, mainly along fault intersections, to form layer-like siliceous rocks and siliceous limestones by depositing Si and Ca. The deposit was formed via interaction between Ge in the fluids and organic matter in the coal seams.

1. Introduction

Germanium (Ge) is a rare element in the Earth's crust with an average concentration of 1.6 ppm (Taylor and McLennan, 1985). It is, however, an important high-technological element widely used in fiber and infrared optics and as polymerization catalysts (Guberman, 2009). Worldwide germanium resources are generally associated with Zn and Pb–Zn–Cu sulfide ores. To a lesser extent, germanium is also recovered from coal ash (Bernstein, 1985; Höll et al., 2007; Guberman, 2008, 2009). Present estimated global resources are only a few thousand tonnes of recoverable Ge and current world refined Ge production (105 tonnes in 2008; Guberman, 2009), can no longer meet the demand of the world market (145 tonnes in 2007). The difference is balanced by recycling (30% of World consumption) and release from existing stockpiles (Guberman, 2008, 2009). It is thus important to continue exploring for new Ge and Ge-bearing ore deposits, as well as gain a better understanding of their origin.

Coal-hosted Ge deposits represent one of the most important Ge or Ge-bearing deposits (Höll et al., 2007). Germanium in coal-hosted Ge deposits is considered to be derived from a variety of sources (Hower et al., 2002). For example, hydrothermal and volcanic activity at Pchelarvo and Vulche Pole (Bulgaria), produced coals extremely enriched in Ge (up to 77,500 ppm on an ash basis; Eškenazy, 1996; Vassilev et al., 1996). Seredin and Danilcheva (2001) attributed this Ge enrichment, with concentrations in excess of 3000 ppm, to deposition resulting from the mixing of N_2-rich alkaline waters with volcanogenic fluids. Infiltration of Ge-enriched water from surrounding sediments has also been proposed as a mechanism for Ge concentration in coals (Minčev and Eškenazi, 1963). Besides the association of Ge with sphalerite (commonly as solid solution within the sulfide) and more rarely silicates, Ge is generally considered to have an organic association in coals (Finkelman, 1982) and tends to concentrate in specific macerals and organic components (Breger and Schopf, 1955; Hallam and Payne, 1958; Krejci-Graf, 1983; Eskenazy, 1996; Vassilev et al., 1996). This suggests that coal seams are favorable for Ge mineralization if there are Ge-rich solutions to interact with them. To date, the role of Ge-rich hydrothermal solutions (fluids) has not been adequately addressed in the literature.

* Corresponding author. Tel.: +86 851 5891962.
E-mail address: huruizhong@vip.gyig.ac.cn (R.-Z. Hu).

0169-1368/$ – see front matter © 2009 Elsevier B.V. All rights reserved.
doi:10.1016/j.oregeorev.2009.02.007

The Lincang Ge deposit, Yunnan, SW China, was discovered in the 1950's during prospecting for uranium (http://www.qqkqw.com/News/V3823.aspx). The deposit, with reserves in excess of 1000 tonnes Ge, is one of the largest coal seam-hosted Ge deposits in the world (Qi et al., 2007). The deposit produced 43% of Chinese Ge in 2007 (http://www.sino-ge.com/index1.asp). Zhuang et al. (1998a) attributed Ge enrichment in the coals of this deposit to weathering of muscovite-bearing granites and adsorption and complexation of Ge by humic acids in the coals. In the present contribution, we summarize the geological and geochemical characteristics of the deposit, focusing on the relationship between hydrothermal activity and Ge mineralization. Finally, we propose a new genetic model in which deposit formation is linked with the hydrothermal activities that also formed the interbedded siliceous rocks and siliceous limestones.

2. Geological background

2.1. Regional geology

From west to east, Southwest China comprises several major tectonic blocks: the Tengchong, Baoshan, Simao and Yangtze Blocks. These are separated from one another by the Lancangjiang–Changning–Menglian and Jinshajiang–Ailaoshan suture zones, respectively (Fig. 1). The Lancangjiang–Changning–Menglian suture zone between the Simao and Baoshan Blocks is marked by dismembered ophiolitic assemblages and Permo-Triassic arc volcanic rocks (Mo et al., 1993). The Jinshajiang–Ailaoshan suture zone was formed as a consequence of collision between the Yangtze Block and Simao Block (Ma, 2002); see also Hou and Cook (2009-this issue).

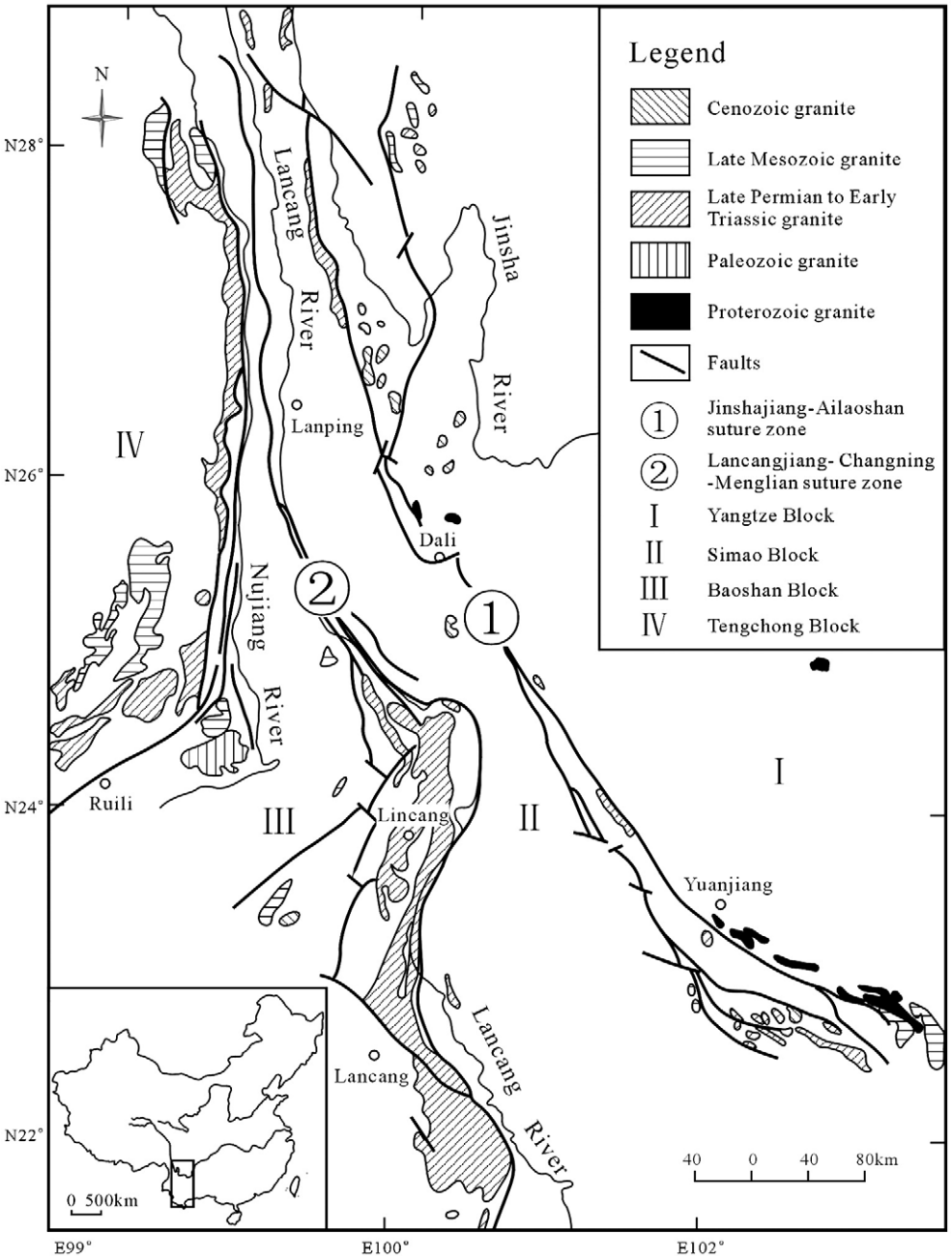

Fig. 1. Distribution of felsic intrusive rocks in West Yunnan, China (after Zhong, 1998). I — Yangtze Block, II — Simao Block, III — Baoshan Block, IV — Tengchong Block.

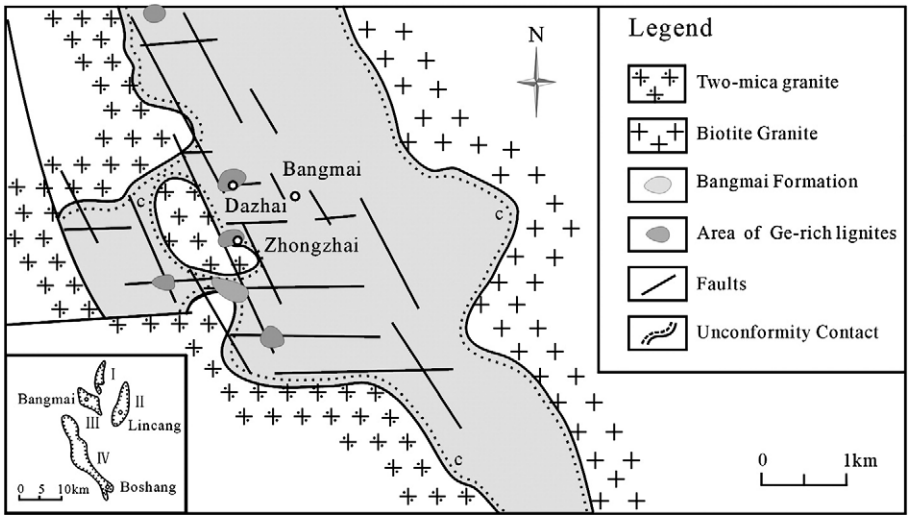

Fig. 2. Simplified geological map of the Bangmai Basin (modified after Hu et al., 1996). I — Mengwang Basin; II — Lincang Basin; III — Bangmai Basin; IV — Mengtuo Basin.

Strata			Thickness (m)	Stratigraphic column	Lithology	Ore Deposit
Quaternary			0~10		Eluvium, slide rock and alluvia	
Miocene	Bangmai Formation	N_{1b}^{8}	0~21		Coarse sandstone	
		N_{1b}^{7}	19~81		Siltstone, argillaceous siltstone with abundant thin ferruginous zone	
		N_{1b}^{6}	11~346		Medium to fine conglomerate, fine sandstone, siltstone, coarse sandstone with 3 to 8 interlayered coal seams. The third coal-bearing unit.	Coal
		N_{1b}^{5}	0~179		Low density diatomaceous siltstone with abundant ferruginous zone	Diatomite
		N_{1b}^{4}	44~263		Fine sandstone, siltstone, coarse sandstone with 6 to 17 interlayered coal seams. The second coal-bearing unit.	Coal
		N_{1b}^{3}	7~95		Conglomerate with interbedded coarse sandstone	
		N_{1b}^{2}	19~364		Coarse sandstone, carboniferous siltstone, siliceous limestone, siliceous rocks with 8 to 14 interlayered coal seams. The basal coal-bearing unit.	Coal and Ge
		N_{1b}^{1}	20~686		Granitic clastic rock (very coarse- grained conglomerate, conglomeratic coarse sandstone, coarse sandstone) with few interlayered fine sandstone and siltstone	
Middle Triassic granite					Medium- to coarse-grained biotite,muscovite and two-mica granites	

Fig. 3. Integrated stratigraphic column for the Bangmai basin (after Qi et al., 2004). The mineralized coal seams interlayered with siliceous rock and limestone occur in the coal seams of the basal coal-bearing unit. The coal seams in the upper two coal-bearing units without siliceous rock and limestone are barren.

Closure of the Paleo-Tethyan Ocean and collision of the Indian and Eurasian plates during the late Permian to early Triassic created the Lancangjiang–Changning–Menlian suture zone (Fig. 1; Zhong, 1998). The Lincang granitic batholiths was emplaced as a result of this collision. The Lincang intrusion is about 350 km long and generally 15 to 45 km wide, and intruded pre-Triassic sedimentary-volcanic rocks. The batholith is dated at ~212 to 254 Ma using zircon U–Pb geochronology (Zhong, 1998) and is overlain by Jurassic strata (Li, 1996).

Lithologically, the Lincang batholith is composed of biotite- and two-mica granites. The rocks consist mainly of K-feldspar, quartz, plagioclase (An_{24-46}), biotite and muscovite. Accessory phases include magnetite, ilmenite, zircon, apatite, monazite and, rarely, allanite, scheelite and cassiterite. The granitic rocks show a calc-alkaline character, with SiO_2 ranging from 65.5 to 74.0 wt.%, and total alkalis (K_2O+Na_2O) from 5.9 to 7.7 wt.%, with $K_2O/Na_2O>1$ (Zhong, 1998). Isotopically, their initial $^{87}Sr/^{86}Sr$ values exceed 0.715 and ε_{Nd} (0) values range from −14.1 to −18.1 (Zhong, 1998). The batholith is considered to have S-type affinity and emplacement relates to collision of the Indosinian and Eurasian plates during the late Permian to early Triassic (Zhong, 1998).

2.2. Geology of the Bangmai Basin

Four basins are recognized in the Lincang district: the Mengwang, Lincang, Bangmai, and Mengtuo basins (Fig. 2). These basins were formed during the Miocene as a consequence of the Himalayan orogeny. They are arranged along NW–SE-trending Tertiary grabens on the Lincang batholith (Fig. 2).

The Bangmai basin, with a surface area of ca. 16 km^2, is an anti-symmetric half graben controlled by NW and EW-trending faults (Fig. 2) and is filled by the Miocene Bangmai Formation with a maximum thickness of 1140 m. The Bangmai Formation was deposited onto the Lincang granitic batholith. The lower part of Bangmai Formation is mainly composed of deluvial–alluvial deposits with granite-derived clastic sediments (N^1_{1b}), overlain by an upper sequence of sandstones, siltstones, coal seams and diatomites of peat swamp-lacustrine-fluvial facies. The upper part is further divided into seven units (Fig. 3). Among the upper seven units, three units are coal-bearing (Fig. 3). The coal seams in these sequences mainly consist of low maturity lignite and a few bituminous coals. Horizontal sequences with fewer and thinner coal seams are found in the eastern limb of the Bangmai Basin. A few sequences with steeply dipping (up to 75°) and thicker coal seams are preserved in the western limb. Coal seams in the basal coal-bearing unit (N^2_{1b}) above the granitic batholith are interbedded with siliceous rocks (cherts) and limestones (Figs. 3 and 4). In contrast, coal seams of the other two coal-bearing units (N^4_{1b} and N^6_{1b}) are interlayered with clastic rocks; siliceous rocks are lacking (Fig. 3). Siliceous rocks and siliceous limestones, probably of hydrothermal origin, are a special feature of Lincang, and are discussed below in detail.

3. Geology of the Lincang Ge deposit

The Lincang Ge deposit, including the Dazhai and Zhongzhai orebodies (Fig. 2), is located in the west part of the Bangmai basin. This deposit has proven Ge reserves of ca. 800 t Ge at Dazhai and at least 200 t Ge at Zhongzhai. Germanium mineralization occurs in the coal seams of the basal coal-bearing unit of the Bangmai Formation. The mineralized coal seam is interlayered with siliceous rocks and siliceous limestones in Zhongzhai, while the other coal seams, which are not interbedded with siliceous rocks and siliceous limestones in the other two units are barren (Figs. 3 and 4). Germanium in the deposit is unevenly distributed in both the vertical and horizontal directions of the coal seams.

The horizontal distribution of orebodies in the Lincang deposit is clearly controlled by faults. The equant or elongated orebodies usually are situated at fault intersections (Fig. 2). These faults penetrate

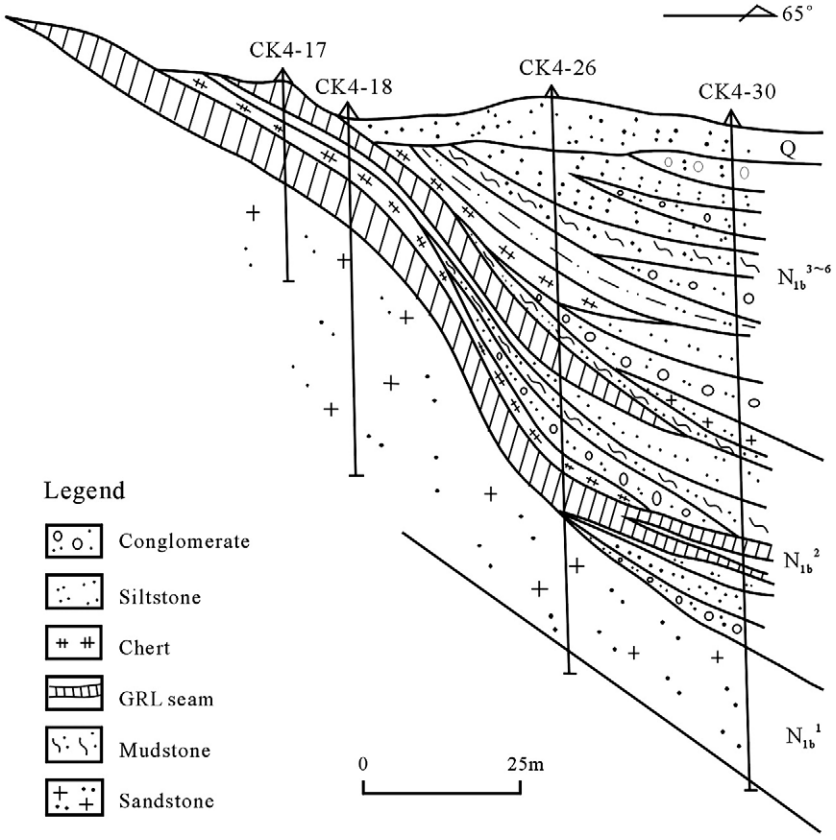

Fig. 4. Geological cross-sections of the Lincang germanium deposit at Zhongzhai (after Hu et al., 1996).

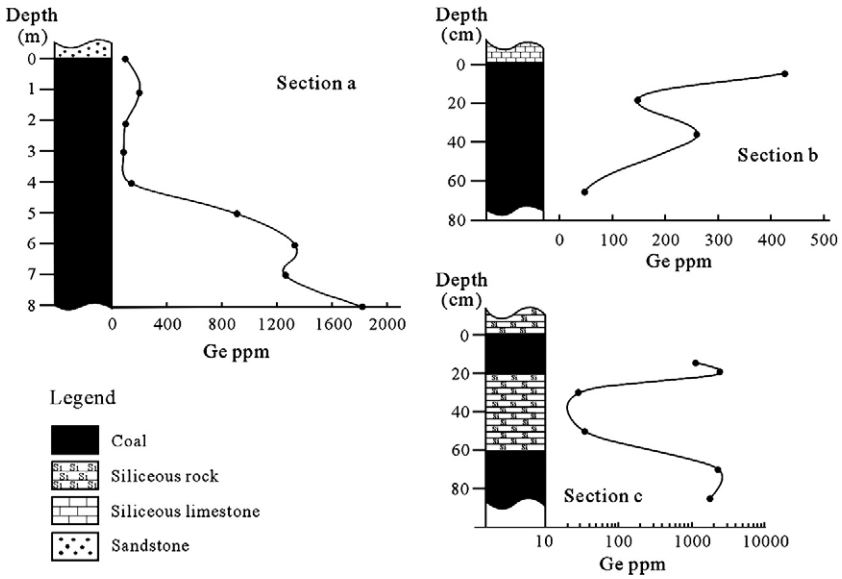

Fig. 5. Ge content *vs.* depth diagrams of the main orebodies of the Lincang germanium deposit (modified after Qi et al., 2004). These sections are located in the underground mine of Dazhai (section A) and Zhongzhai (sections B and C). Ge can be concentrated at bottom, top of coal seam or where coal seams are in contact with siliceous rocks or siliceous limestones.

upwards from the granite batholith to the strata of the basal coal-bearing unit, and are considered to be contemporaneous structures developed during the time of sedimentation.

The mineralized area in Dazhai is 600 m long and 400 m wide, with an area of 0.25 km^2. The stratiform or lentiform orebodies, with an average thickness of 4 m (up to 14.3 m), measure 470 m × 400–800 m in area (Li, 2000). Germanium in the mineralized coal seams is mainly associated with organic matter, with Ge grades ranging from a few tens of ppm to about 2500 ppm, with an average of ca. 850 ppm (Qi et al., 2004).

Germanium appears to be concentrated at the top and bottom of coal seams, where coal seams are in contact with siliceous rocks or siliceous limestones (Fig. 5). In cross-section A, the coal seams at Dazhai are about 10 m in thickness with sandstones in the hanging wall and siltstones in the footwall. Ge contents of coal seams in this section vary from 78 to 1800 ppm. Germanium is notably concentrated in the lower portion of the coal seams, while the upper portions (in contact with sandstone) are relatively Ge-poor. In cross-section B, the coal seams of Zhongzhai contain 35 to 435 ppm Ge with siliceous limestone as hanging wall rock and sandstone as footwall rock. Here, Ge is clearly concentrated in the upper portion of the coal seam, which is in contact with siliceous limestones. In cross-section C, Ge in the coal seams of Zhongzhai, with Ge contents from 1100 to 2500 ppm, is also richer towards the siliceous rocks.

No discrete Ge minerals have been observed in the deposit. Germanium in mineralized coal seams is mainly associated with organic matter (Zhuang et al., 1998b). Results of heavy media separation show that Ge occurs predominantly in huminites, including 86 to 89% in corpohuminites and 2 to 10% in light macerals. Another 2 to 10% Ge is absorbed in various organic matter (Zhuang et al., 1998b). The TEM-EDX analyses also reveal the existence of Ge in huminites, in which C, O, Si, Al, S, Ca, Cu and Fe are detected (Fig. 6).

4. Geochemistry of the Lincang Ge deposit

4.1. Hydrothermal origin of sedimentary siliceous rocks and limestones

The siliceous rocks (cherts) are usually distributed as interlayers with the mineralized coal seams in Zhongzhai. They are mainly bedded or lensoid in shape, gray-black in color, and range from 20 to 60 cm in thickness. These rocks mainly display cryptocrystalline textures (Fig. 7A), and locally exhibit zonal micro-textures (Fig. 7B–I), obviously different from sedimentary clastic quartz. The peripheral portions of the zonal textures consist of radiating chalcedony with undulatory extinction, while the middle portions consists of idiomorphic quartz, very similar to those of so-called “mammillary

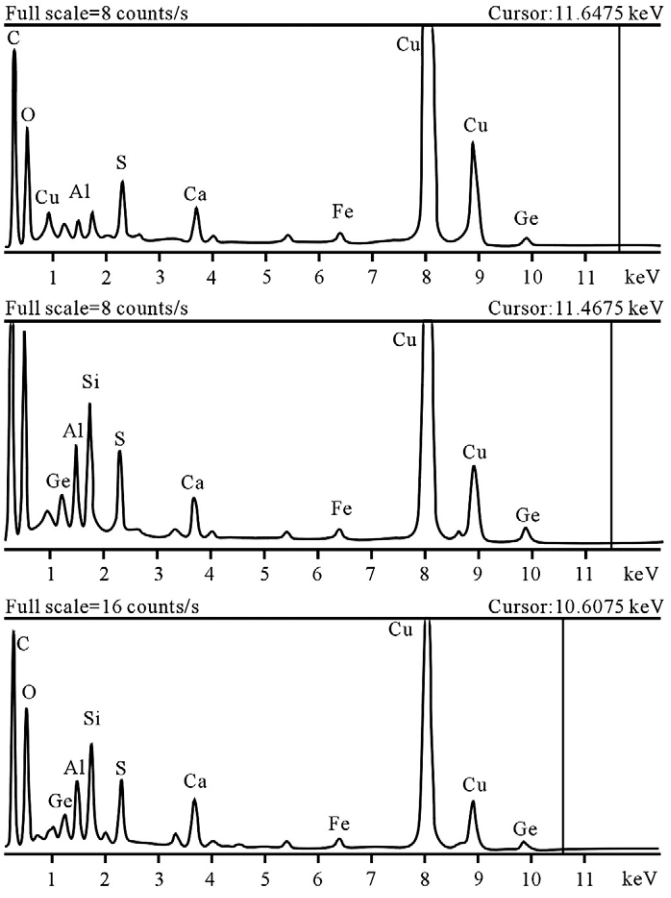

Fig. 6. Selected TEM-EDX spectrums for huminites in Ge-rich lignite from the Lincang germanium deposit. Two Ge peaks were identified, indicating that Ge is mainly concentrated in huminite. The Cu peaks result from the copper grid used during the sample analysis.

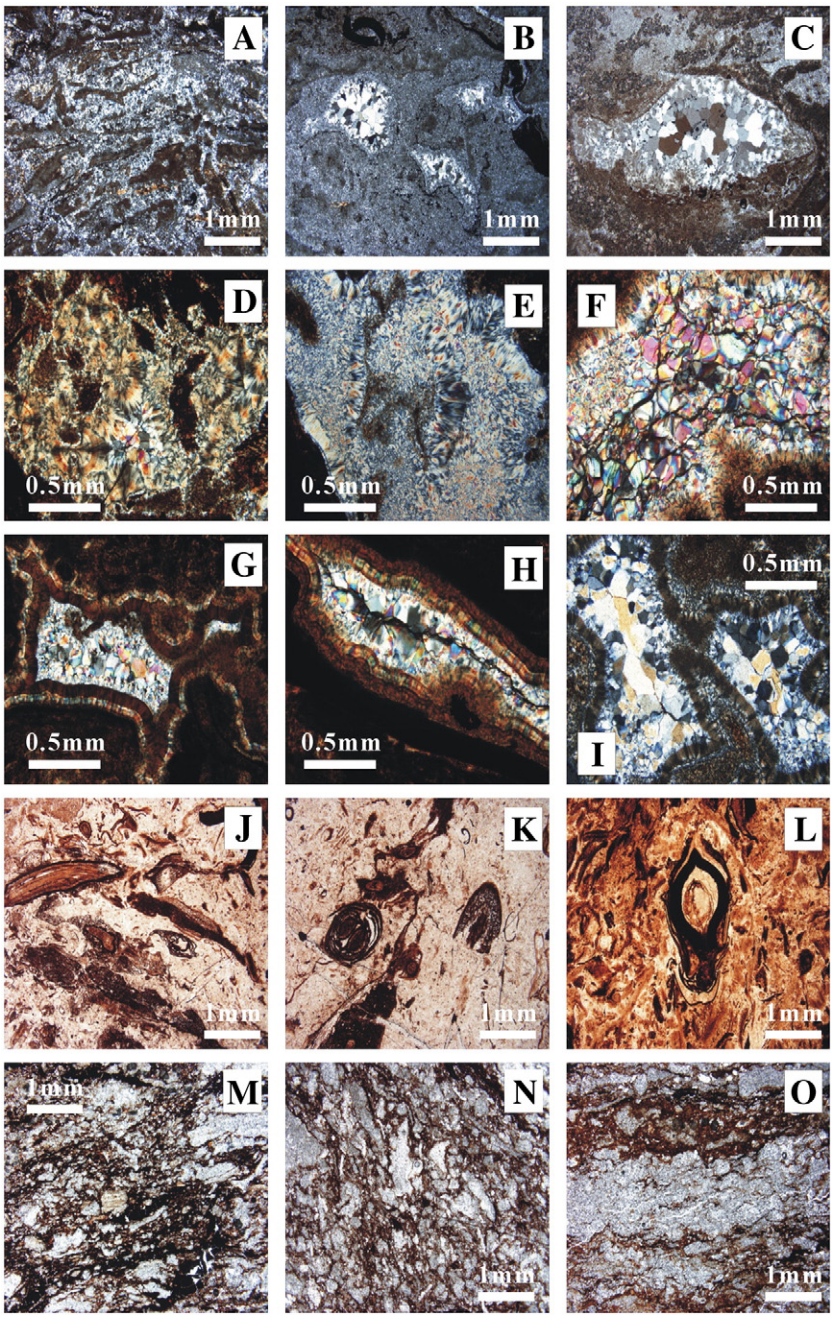

Fig. 7. Photomicrographs of thin-sections of siliceous rocks (A–L) and siliceous limestone (M–O). A. Silicified fossils in a very fine-grained silica groundmass, cross polarized light; B–I. Zonal textures or original cavities in siliceous rocks filled with different form silica: radiating chalcedony usually distributed in peripheral portions, while coarse quartz grains set in the central part, cross polarized light; J–L. Various fossil plant fragments in siliceous rocks, plain light; M–N. Amorphous calcites cemented by dark organic matters; O. laminated texture of siliceous limestone.

texture" which had been regarded as the main lithological features of hydrothermal sediments (Tu, 1988; Chen and Chen, 1990). Similar textures also can be found in the hydrothermal cherts from Hunan, China (Chen et al., 2009). Fossil plant fragments in the banded siliceous rocks are noted (Fig. 7J–L). Pyrites in these rocks are generally cubic, and their aggregations show framboidal shape.

Siliceous limestones in the deposit are also interbedded with the mineralized coal seams. They generally range from 10 to 30 cm in thickness, with gray-brown color and low rock density (Qi et al., 2004). The siliceous limestones mainly consist of irregular grains of amorphous calcite, which are cemented by dark organic matter (Fig. 7M–N). Locally, the thin layers of organic matter are interlayed by 'pure' amorphous calcite (laminated texture, Fig. 7O).

4.1.1. Major elements

The interbedded siliceous rocks in the deposit have very high SiO_2 contents ranging from 84.3 to 97.6 wt%, with an average of 92.8 wt%. Their TiO_2 and Al_2O_3 contents vary from 0.001 to 0.02 wt.% (with an average of 0.01 wt.%), and from 0.01 to 0.03 wt.% (with an average of 0.02 wt.%), respectively (Table 1). The Al/(Al + Fe + Mn) ratios of siliceous rocks in the deposit vary from 0.004 to 0.028 (with an average of 0.010). These values are comparable to hydrothermal cherts reported from elsewhere in the world (Boström et al., 1979; Adachi et al., 1986; Yamamoto, 1987).

The siliceous limestones in the deposit are chiefly composed of CaO and CO_2, with total (CaO + CO_2) ranging from 79.5 to 90.1 wt.%, which is relatively lower than those (93.5%–94.0 wt.%) of laminated

Table 1
Major element compositions of the siliceous rocks and siliceous limestones from the Lincang germanium deposit (LGD) and comparison with other sediments (wt.%).

Rock	Sample	SiO_2	TiO_2	Al_2O_3	Fe_2O_3	FeO	MnO	MgO	CaO	Na_2O	K_2O	P_2O_5	LOI	Total	Na_2O/K_2O	Al//(Al + Fe + Mn)
Siliceous rock, LGD	ZZ-19	84.31	0.01	0.01	1.00	0.20	0.06	0.11	0.20	0.12	0.02	0.08	13.31	99.43	3.58	0.006
	ZZ-27	96.75	0.02	0.02	0.60	0.12	0.07	0.10	0.20	0.11	0.02	0.12	1.50	99.63	3.28	0.018
	ZZ-38	97.60	0.01	0.03	0.86	0.10	0.07	0.10	0.40	0.11	0.01	0.11	0.26	99.66	6.56	0.021
	ZZ-45	96.39	0.001	0.01	0.75	0.15	0.11	0.10	0.50	0.12	0.03	0.11	1.50	99.77	2.39	0.007
	ZZ-57	89.83	0.001	0.01	0.54	0.10	0.07	0.10	0.20	0.11	0.04	0.15	8.70	99.85	1.64	0.010
	ZZ-61	95.52	0.002	0.02	1.32	0.32	0.10	0.11	0.10	0.12	0.03	0.08	1.60	99.32	2.39	0.008
	ZZ-74	95.60	0.02	0.01	0.39	0.10	0.06	0.10	0.10	0.11	0.04	0.07	3.20	99.80	1.64	0.013
	ZZ-79	96.09	0.01	0.02	0.72	0.20	0.08	0.11	0.20	0.12	0.03	0.03	2.10	99.71	2.39	0.014
	ZZ-81	89.06	0.001	0.02	0.70	4.70	0.20	0.11	0.70	0.11	0.02	0.15	4.06	99.83	3.28	0.002
	ZZ-87	86.59	0.003	0.01	1.32	0.30	0.08	0.10	4.60	0.10	0.02	0.07	6.35	99.54	2.98	0.004
	Average	92.77	0.01	0.02	0.82	0.63	0.09	0.10	0.72	0.11	0.03	0.10	4.26	99.65	3.01	0.011
Siliceous rock, WQL[a]		95.30	0.04	0.41	1.03	0.58	0.03	0.19	0.68	0.06	0.08	0.25	1.06	99.71	0.45	0.211
Siliceous rock, Franciscan[b]		92.30	0.09	1.31	0.27	2.36	0.53	0.28	0.11	0.16	0.35	0.03			0.27	0.222
Siliceous rock, Shimanto[c]		87.87	0.05	1.09	0.52	2.52	1.08	0.86	1.05	0.35	0.24	0.12			0.87	0.154

	Sample	SiO_2	TiO_2	Al_2O_3	Fe_2O_3	FeO	MnO	MgO	CaO	Na_2O	K_2O	P_2O_5	CO_2	LOI	Total		
Siliceous limestone, LGD	ZZ-58	6.43	0.06	0.01	0.90	0.30	0.11	0.40	46.90	0.16	0.03	0.16	35.05	9.10	99.61	3.18	0.006
	ZZ-60	8.31	0.01	0.02	0.26	0.10	0.12	0.41	48.60	0.15	0.07	0.10	35.91	5.67	99.78	1.28	0.029
	ZZ-77	5.05	0.06	0.01	0.15	0.05	0.09	0.30	45.00	0.15	0.06	0.12	34.47	14.10	99.61	1.49	0.024
	ZZ-84	4.94	0.02	0.02	0.73	0.10	0.29	0.60	52.50	0.15	0.02	0.10	37.62	2.60	99.69	4.47	0.013
	ZZ-91	5.78	0.01	0.01	1.61	0.40	0.30	0.50	49.90	0.14	0.02	0.09	37.16	4.05	99.97	4.17	0.003
Travertine, Tengchong[d]	S2	0.34	–	0.03	–	2.83	0.12	2.95	51.99	0.08	0.03	–	41.48	0.14	99.99	1.59	0.007
	SK94	1.31	–	0.02	–	0.33	0.92	2.56	53.64	0.59	0.02	–	40.40	0.41	100.20	17.59	0.011
Marine limestone, Guiyang[e]	H-1	4.47	0.32	0.47	0.62	0.10	0.001	1.20	52.10	0.12	0.42	0.37	38.70	0.45	99.34	0.17	0.327
	H-2	3.23	0.05	0.71	0.74	0.15	0.02	1.40	53.20	0.13	0.26	0.30	39.10	0.50	99.79	0.30	0.366
	H-3	4.18	0.08	0.23	0.53	0.10	0.01	1.50	52.25	0.12	0.25	0.13	39.00	1.05	99.43	0.29	0.211
	H-4	4.57	0.18	0.47	0.45	0.09	0.02	1.40	52.70	0.12	0.23	0.05	39.05	0.60	99.93	0.31	0.383
	H-5	6.44	0.32	0.23	2.00	0.39	0.03	1.50	51.95	0.13	0.26	0.30	35.10	0.70	99.35	0.30	0.066

– Signifies element not detected. Data of siliceous rocks and limestones after Qi et al. (2002a, 2004).
[a] WQL.
[b] Franciscan.
[c] Shimanto (average composition of hydrothermal cherts from the West Qinling, Franciscan and Shimanto terranes, respectively). Data of WQL after Liu et al. (1999), Franciscan and Shimanto after Yamamoto (1987).
[d] Data after Wang et al. (1998).
[e] Data after Sun (2002); LOI: loss on ignition.

Quaternary hydrothermal travertine from Tengchong hydrothermal area, Yunnan, China. The Al/(Al + Fe + Mn) ratios of siliceous limestones in the deposit varies from 0.002 to 0.021 (with an average of 0.011), basically similar to the Tengchong travertine (0.010–0.016), but much lower than those (0.066–0.383, 0.271 on average) of normal Lower Triassic marine limestones from Guiyang, China (Table 1).

4.1.2. Trace elements

According to Rona (1984), normal sedimentary rocks have Th contents higher than U, while hydrothermal sedimentary rocks have U contents higher than Th. U/Th ratios of the siliceous rocks and siliceous limestones from the deposit are much greater than 1 (Table 2). In the $U_{vs.}$ Th diagram (Boström et al., 1979; Rona, 1984), the siliceous rocks and limestones also fall into hydrothermal fields (Fig. 8).

Low total REE contents and left-inclined North American Shale Composition (NASC)-normalized REE patterns are considered as common features of hydrothermal cherts (Crerar et al., 1982; Marchig et al., 1982). The ΣREE content of the siliceous rocks from Lincang are very low, varying only from 0.20 to 2.32 ppm. Their NASC-normalized REE patterns are flat or left-inclined (Fig. 9A), basically similar to those of both hydrothermal cherts (Marchig et al., 1982; Yamamoto, 1987; Kunzendorf et al., 1988; Murray et al., 1990) and thermal springs associated with the Idaho granitic batholith (Middlesworth and Wood, 1998). It is worth pointing out that the Lincang siliceous rocks show no negative Ce anomalies (Ce/Ce* = 0.997 to 1.174). Negative Ce anomalies usually appear in marine hydrothermal cherts or sediments (Marchig et al., 1982; Yamamoto, 1987; Kunzendorf et al., 1988; Murray et al., 1990). Murray et al. (1990) found that Ce anomalies of interbedded cherts and shales were connected with their depositional regimes; cherts and shales influenced by continental input show no or only slight Ce anomalies (Ce/Ce* = 0.90 to 1.30). Thus, the lack of Ce anomalies may be attributed to a continental environment for the formation of the siliceous rocks from Lincang.

The siliceous limestones from Lincang have low total REE contents (<5 ppm) and left-inclined NASC-normalized REE patterns similar to Tengchong hydrothermal travertines (Fig. 9B). In contrast, the REE compositions of the Lincang siliceous limestones are clearly distinguished from normal marine limestones from Guiyang. The Guiyang limestones have ΣREE contents about one magnitude higher than the Lincang limestones (Table 2), as well as flat or slightly right-inclined patterns (Fig. 9C) that are clearly different from the Lincang limestones.

4.1.3. Oxygen and carbon isotopes

$\delta^{18}O_{SMOW}$ values of 11 Lincang siliceous rock samples vary from 10.9 to 15.7‰ with an average of 13.5‰ (Table 3), different from those of volcanic (1.9 to 12.4‰; Liu et al., 1999) and biochemical (21.6 to 26.7‰; Yao et al., 2002) siliceous rocks, but similar to those of hot-spring siliceous sinter (12.2 to 23.6‰; Clayton, 1986). $\delta^{18}O_{SMOW}$ and $\delta^{13}C_{PDB}$ values of 3 Lincang siliceous limestone samples range from 18.0 to 18.7‰ and 6.1 to 6.9‰, respectively, which are also similar to those of modern hydrothermal travertine (Table 3).

4.2. Mineralized and barren coal seams

Ge-rich lignites in Lincang are mainly half-bright and half-dull coal with banded or massive structure, and consist of huminite, intertinite,

Table 2
Trace element and REE concentrations of different rocks from the Lincang germanium deposit (ppm).

Element	UCC[a]	GRL[b] in Dazhai (52)[c]				GFL[e] in Zhongzhai (5)				SR[f](10)		SL[g](5)		TMG[h] (3)	
		Min	Max	Aver.	EF[d]	Min	Max	Aver.	EF	Aver.	EF	Aver.	EF	Aver.	EF
Li	20	0.65	19.2	7.30	0.37	0.38	2.25	0.91	0.05	8.29	0.41	9.85	0.49	33.2	1.66
Sc	11	0.003	7.10	1.76	0.16	0.06	1.14	0.65	0.06	0.28	0.03	0.35	0.03		
V	60	2.94	26.3	10.7	0.18	5.66	13.3	10.7	0.18	2.82	0.05	0.82	0.01	11.3	0.19
Cr	35	3.82	128	18.1	0.52	10.2	13.8	12.3	0.35	13.4	0.38	2.68	0.08	75.7	2.16
Co	10	3.84	57.2	18.0	1.80	13.6	220	92.3	9.23	2.20	0.22	1.77	0.18	11.1	1.11
Ni	20	1.95	194	14.9	0.75	6.83	27.5	17.7	0.89	5.82	0.29	7.63	0.38	11.6	0.58
Cu	25	6.59	44.3	13.7	0.55	6.37	11.7	9.61	0.38	9.20	0.37	4.68	0.19	12.1	0.48
Zn	71	7.03	244	41.3	0.58	3.61	26.9	15.8	0.22	5.02	0.07	15.2	0.21	43.5	0.61
Ga	17	1.07	16.3	4.63	0.27	0.78	1.70	1.20	0.07	0.60	0.04	0.50	0.03	22.5	1.32
Ge	1.6	25.5	2523	852	533	0.54	0.78	0.64	0.40	78.4	49.0	66.7	41.7	3.4	2.13
As	1.5	0.81	410	47.6	31.7	6.57	618	264	176	11.0	7.32	2.32	1.55	17.9	11.9
Rb	112	4.88	74.9	28.8	0.26	3.70	15.4	7.93	0.07	2.75	0.02	3.32	0.03	–	–
Sr	350	10.1	45.6	24.3	0.07	26.2	35.2	30.2	0.09	4.66	0.01	606	1.73	10.6	0.03
Y	22	1.45	68.9	10.4	0.47	7.13	12.4	9.84	0.45	0.33	0.02	0.74	0.03	21.7	0.99
Zr	190	3.48	764	29.5	0.16	3.70	7.54	6.14	0.03	1.49	0.01	1.82	0.01	42.4	0.22
Nb	25	0.53	315	46.8	1.87	0.39	0.78	0.67	0.03	9.75	0.39	2.25	0.09	21.4	0.86
Mo	1.5	0.93	15.1	5.46	3.64	2.70	7.57	4.88	3.25	1.59	1.06	0.30	0.20	4.97	3.31
Cd	0.098	0.06	2.64	0.51	5.18	0.07	0.12	0.10	1.02	0.06	0.63	0.07	0.67	0.45	4.59
Sn	5.5	0.78	16.4	4.23	0.77	0.78	1.58	1.26	0.23	1.49	0.27	1.39	0.25	21.9	3.98
Sb	0.2	0.81	347	32.8	164	1.74	2.40	2.08	10.4	8.21	41.0	16.2	81.2	26.8	134
Cs	3.7	3.73	75.1	22.7	6.13	1.51	6.21	3.10	0.84	4.91	1.33	2.35	0.64	–	–
Ba	550	36.9	1023	105	0.19	119	170	144	0.26	105	0.19	1523	2.77	52	0.09
Hf	5.8	0.50	4.70	1.87	0.32	0.15	0.49	0.32	0.06	0.05	0.01	0.15	0.03	–	–
Ta	2.2	0.05	2.33	0.39	0.18	0.03	0.07	0.05	0.02	0.02	0.01	0.05	0.02	–	–
W	2	109	975	378	189	11.9	79.5	41.9	21.0	9.52	4.76	29.5	14.7	11.9	5.95
Tl	0.75	0.04	16.23	1.62	2.16	0.02	2.60	1.28	1.71	0.43	0.57	0.16	0.21	2.93	3.91
Pb	20	2.14	47.0	11.2	0.56	2.25	5.68	3.74	0.19	0.96	0.05	1.25	0.06	56.9	2.85
Bi	0.127	0.06	4.89	1.21	9.51	0.05	0.14	0.08	0.63	0.03	0.23	0.02	0.17	4.56	35.9
Th	10.7	0.47	12.4	4.15	0.39	2.10	3.64	2.81	0.26	0.12	0.01	0.23	0.02	–	–
U	2.8	1.05	640	56.0	20.0	0.82	3.56	2.18	0.78	2.05	0.73	0.65	0.23	–	–
La	30	1.16	23.0	4.53	0.15	6.49	7.83	7.38	0.25	0.164	0.005	0.600	0.020	15.4	0.51
Ce	64	1.94	60.8	11.0	0.17	14.5	20.2	17.6	0.28	0.320	0.005	0.893	0.014	32.5	0.51
Pr	7.1	0.16	5.23	1.10	0.15	1.36	1.96	1.71	0.24	0.029	0.004	0.059	0.008	4.32	0.61
Nd	26	0.03	19.7	3.48	0.13	4.65	7.52	6.35	0.24	0.110	0.004	–	–	15.7	0.60
Sm	4.5	0.19	5.99	1.20	0.27	1.14	1.99	1.64	0.36	0.028	0.007	0.079	0.018	4.27	0.95
Eu	0.88	0.02	0.59	0.13	0.15	0.17	0.30	0.24	0.27	0.011	0.011	0.046	0.053	0.27	0.31
Gd	3.8	0.18	8.01	1.22	0.32	1.19	2.06	1.67	0.44	0.025	0.008	0.084	0.022	3.19	0.84
Tb	0.64	0.03	1.67	0.25	0.39	0.19	0.34	0.26	0.41	0.005	0.008	0.014	0.022	0.48	0.75
Dy	3.5	0.19	10.3	1.59	0.45	1.00	1.89	1.50	0.43	0.031	0.009	0.106	0.030	2.62	0.75
Ho	0.8	0.04	1.87	0.32	0.40	0.20	0.40	0.30	0.38	0.007	0.013	0.022	0.027	0.44	0.55
Er	2.3	0.12	5.01	0.99	0.43	0.60	1.15	0.90	0.39	0.022	0.009	0.075	0.033	1.36	0.59
Tm	0.33	0.02	0.73	0.16	0.48	0.08	0.16	0.12	0.36	0.004	0.012	0.009	0.028	0.19	0.58
Yb	2.2	0.12	5.3	1.14	0.52	0.51	1.06	0.81	0.37	0.027	0.014	0.070	0.032	1.55	0.70
Lu	0.32	0.02	0.83	0.16	0.50	0.08	0.14	0.11	0.34	0.005	0.016	0.011	0.034	0.21	0.66

– Signifies that the element was not analyzed or is at concentration below the detection limit. Data after Qi et al. (2002b, 2004 and unpublished).
[a] Average composition of upper continental crust (UCC) after Taylor and McLennan (1985).
[b] Ge-rich lignite (GRL).
[c] Number of analyses.
[d] Enrichment factor (EF) = X_{aver}/X_{UCC}.
[e] Ge-free lignite (GFL).
[f] Siliceous rock (SR).
[g] Siliceous limestone (SL).
[h] Two-mica granite (TMG).

liptinite and inorganic components. Huminite generally makes up 60 to 80% of the lignites. Intertinite includes mainly fusovitrite, and comprises about 2 to 10% of the lignite. Liptinite is composed of cutinitem, resinite, small sporinite, alginite and funginite, and accounts for about 2 to 3% of the lignites. Inorganic components are mainly clay minerals and constitute ca. 5 to 10% of the lignites. Ge-free lignites are lithologically similar to Ge-rich lignites, although their huminite content is usually <70%, lower than those of Ge-rich lignites (Han et al., 1994; Zhuang et al., 1998a).

4.2.1. Trace elements

Ge-rich lignites are distinctly enriched in Ge, Sb, W, U, and Bi relative to the upper continental crust (UCC) (Taylor and McClennan, 1985) (Table 2, Fig. 10). In comparison with Ge-free lignites, Ge-rich lignites are almost always enriched in most trace elements, particularly Ge, Nb, Li, Sb, W, Bi, and U (Table 2, Fig. 11). The enrichment of these elements is similar to the Spetsugli coal-hosted Ge deposit, Russia (Seredin, 2003, 2005). The Spetsugli deposit is also located in a Tertiary coal-bearing basin underlain by Ge-enriched granites. Trace element enrichment in the Ge-rich coal seams, compared with those in Ge-free coal seams, was considered to result from influx of these elements from Ge-bearing hydrothermal fluids (Seredin, 2003, 2005).

The total REE content of Ge-rich lignites varies from 5.1 to 148 ppm, and of Ge-free lignites from 32.2 to 46.8 ppm. NASC-normalized REE patterns of Ge-free lignites from the Lincang Ge deposit are flat (Fig. 9D). The REE patterns of Ge-rich lignites show variation; with increasing Ge contents the REE patterns appear HREE-enriched (Fig. 9E). The HREE enrichment in Ge-rich lignites is even more distinct if their REE contents are compared to the average compositions of Ge-free lignites. Ge-rich lignites with Ge contents of <200 ppm are nearly flat; as Ge increases, however, HREE are substantially enriched (Fig. 9F) such that there is a clear correlation

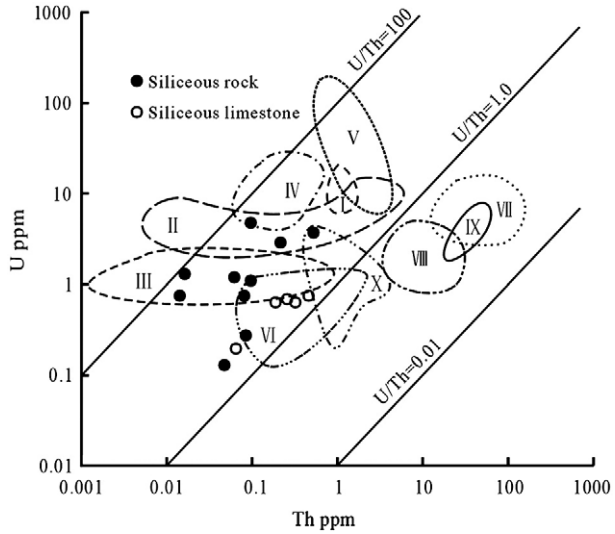

Fig. 8. U–Th diagram of various sediments (after Boström et al., 1979; Rona, 1984). I — TAG hydrothermal area; II — Galapagos spreading center deposits; III — Amphitrite hydrothermal sediments; IV — Red Sea hot brine deposits; V — East Pacific Rise crest deposits; VI — Långban hydrothermal sediments; VII — Ordinary manganese nodules; VIII — Ordinary pelagic sediments; IX — Laterites; X — Fossil hydrothermal deposits (En Kafala ores). The siliceous rocks and limestones from Lincang Germanium Deposit fall into the hydrothermal sedimentary field.

between LREE/HREE ratio and Ge content (Fig. 12). NASC-normalized REE patterns of normal coal seams are usually flat, whereas the patterns of coal seams reworked by hydrothermal fluids are relatively enriched in HREE (Wu et al., 1994; Chen et al., 1996; Seredin, 2005). HREE enrichment in Ge-rich lignites demonstrates that the REE content reflect comparable REE sources as for the Ge-free lignite, but this is superimposed by an additional REE influx from hydrothermal fluids.

4.2.2. Sulfur isotopes

Ge-rich lignites in the basal coal-bearing unit contain disseminated pyrites with δ^{34} S values ranging from 17.2 to 51.4‰ (Table 4, Fig. 13), indicating that these pyrites are of 'normal' sedimentary origin. Thin vein-like pyrites, on the other hand, have δ^{34}S values from 1.9 to −5.4‰, similar to those of the sulfides (pyrite, sphalerite, chalcocite and galena) in quartz veins within the basement granites (Table 4, Fig. 13). This suggests that granite-related material has contributed as a sulfur source. δ^{34}S values of pyrite in the Ge-free lignites from other coal-bearing units vary from 18.6 to 28.6‰, again attributable to a normal sedimentary origin.

5. Discussion

5.1. Contribution from coal-forming plants

Research has been carried out on the origin of Ge in coals since Goldschmidt and Peters (1933) noted that some coals were Ge-enriched. In previous studies, two models were proposed to explain the origin of Ge-rich coal seams. The syngenetic model suggests that Ge in coals was inherited from coal-forming plants, whereas the epigenetic model attributed Ge in coals to scavenging, by the coals, from Ge-enriched water circulating in the surrounding sediments during the process of coal formation or at some time thereafter (Minčev and Eškenazi, 1963; Ratynskiy et al., 1966).

The epigenetic model has received considerable support from many observations. Although plants are able to absorb and concentrate Ge from both the air and soil, superfluous Ge will generally inhibit plant growth and even poison the plants (Bernstein, 1985). It is known that plant ashes generally contain very low Ge (<10 ppm; Weber, 1973) and that only a small proportion of coal seams worldwide are rich in Ge (Seredin and Danilcheva, 2001). Coal seams derived from plants of the same era and the same growing environment often show great diversities in their Ge concentrations (Hu et al., 1996). In mineralized coal seams, Ge concentrations are generally negatively related to their thickness (Kulinenko, 1977). Furthermore, the Ge distribution is usually uneven across the section and tends to be concentrated at the top and bottom of coal seams (Yudovich, 2003; this work). Smivnov (1977) demonstrated that Ge concentrations in coal seams were commonly related to the permeability of the country rocks; country rocks with relatively high permeability favoring Ge enrichment. Based on these observations, it is reasonable to assume that Ge in coal seams is dominantly derived from an external source during or after coalification, rather than from the coal-forming plants themselves (Minčev and Eškennazi, 1963; Eškennazi, 1996; Hu et al., 1996, 1999; Zhuang et al., 1998a; Seredin and Danilcheva, 2001; Hower et al., 2002; Qi et al., 2004; Höll et al., 2007).

5.2. Coal seams as favorable host rocks for Ge mineralization

Germanium was thought to have an organic association in coals and tends to concentrate in specific macerals and organic components (Breger and Schopf, 1955; Hallam and Payne, 1958; Finkelman, 1982; Krejci-Graf, 1983; Vassilev et al., 1996; Eškenazy, 1996; Zhuang et al., 1998a). Germanium-enriched coals are generally woody lignites (Weber, 1973; Smirnov, 1977; Hu et al., 1996; Qi et al., 2004). Besides lignite, peats and other types of organic sediments are also able to enrich Ge (Kulinenko, 1977; Zhang et al., 1987; Qi et al., 2005). Experiments on the interaction between coals and Ge-bearing solutions show that complexation of Ge with coal humus can be as high as 8000 ppm (Zhang et al., 1987), i.e., much higher than the normal values (generally from $n\times10$ to $n\times100$ ppm) in natural mineralized coal seams. This might indicate that the humus in coal has much greater ability to concentrate Ge than is observed naturally. Zhang et al. (1987) pointed out that Ge contents in coals do not correlate directly with the content of humus in coals, because the abundance of humus in coals is actually much higher than that of humus complexed with Ge in geological systems. As a result, the Ge content is considered unlikely to increase limitlessly with increasing humus content due to the limited Ge sources. In contrast, even when humus contents in coals are relatively low, they are high enough to scavenge Ge from solution. It is generally accepted that the humus in all kinds of coals are able to fix Ge from surrounding water under favorable conditions such as temperature, pH and Eh. Coal seams are thus favorable host rocks for Ge mineralization (Hu et al., 1999).

5.3. Solubility of Ge in hydrothermal fluids

An epigenetic origin for Ge in coals requires the element to be transported in fluids. In natural water, organic Ge is stable, and thus does not participate in the geochemical cycle (Lewis et al., 1985). Therefore, Ge occurs as inorganic species in solution, at least before it infiltrates coals. Germanium concentrations in natural water are extremely low (typically <1 ppb, Arnórsson, 1984), which is probably the reason why most coals in the world are not enriched in Ge. For example, although a series of Miocene coal-bearing basins occur above basement rocks with elevated concentration of Ge in the west of Yunnan province, only a few are Ge-enriched. It is therefore possible that coals can be enriched in Ge if they interact with inorganic Ge-enriched solution during or after coalification. Thus, Interaction between inorganic Ge-rich solution and coal seams is a key factor controlling Ge enrichment in coal seams.

Recent studies on Ge and Si in natural waters (ocean, surface waters, continental geothermal systems and mid-ocean ridge hydrothermal solutions) reveal that even under room or lower temperature

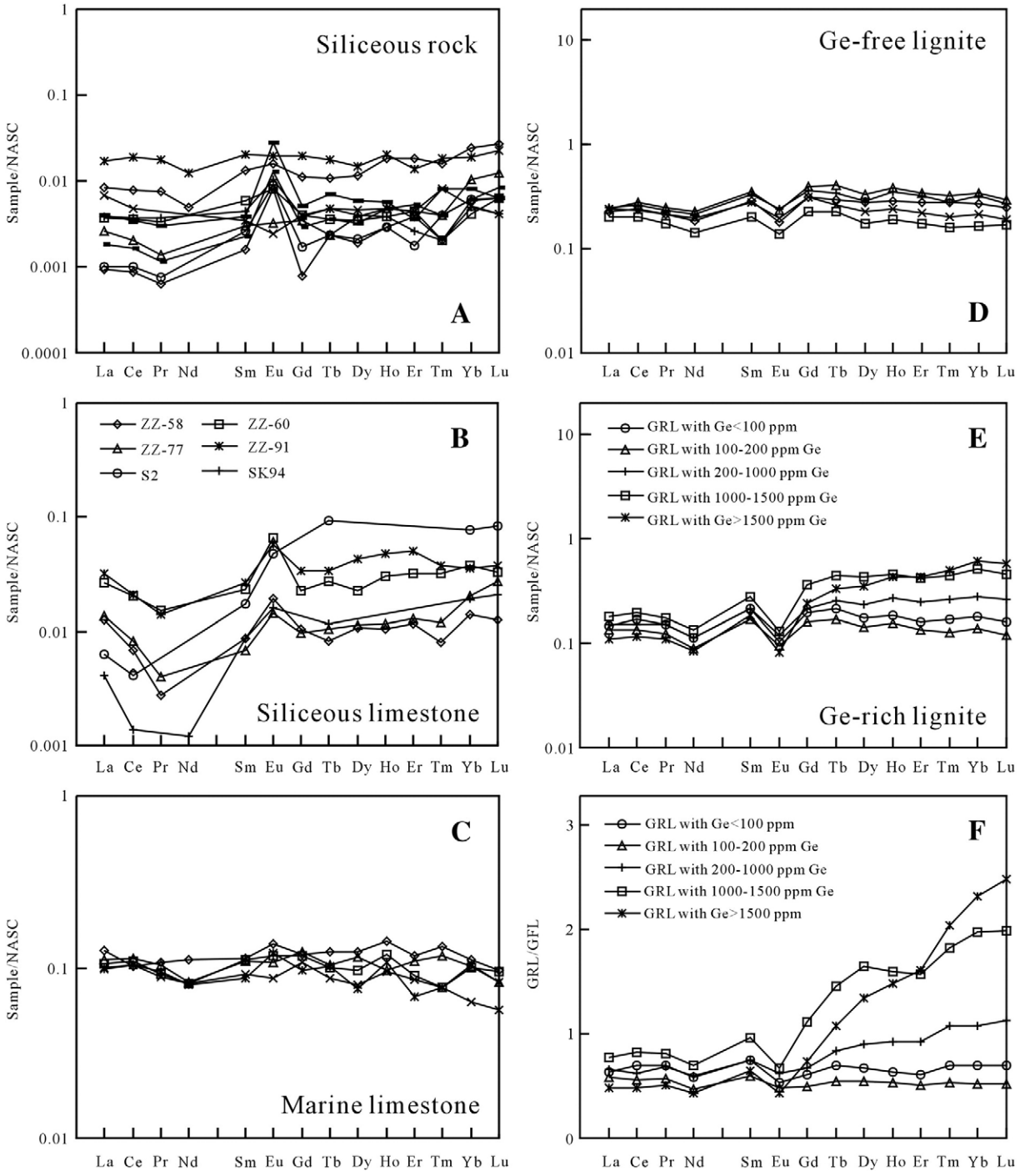

Fig. 9. (1) NASC-normalized REE patterns of the siliceous rocks (A), siliceous limestones (B), Ge-free lignites (D) and Ge-rich lignites (E) from the Lincang Ge deposit, as well as marine limestone (C) from Guiyang, China (REE data after Sun, 2000 unpublished). (2) Ge-free lignite (GFL)-normalized REE patterns of Ge-rich lignites (GRL) with various Ge contents from the Lincang deposit (F). S2 and SK94 in B are travertine from the Tengchong hydrothermal area (REE data after Wang et al., 1998). The siliceous rocks and limestones show slight but distinct enrichment of HREE, different from those of marine limestone. HREE enrichment with increasing Ge content in Ge-rich lignite. REE data of NASC are from Taylor and McLennan (1985).

conditions, Ge has inorganic chemical features similar to Si (Pokrovski and Schott, 1998a,b). The solubilities of Ge and Si in solutions are positively related to temperature (Pokrovski and Schott, 1998b). Germanium contents in continental geothermal fluids (Arnórsson, 1984) and present-day mid-ocean ridge hydrothermal fluids (Mortlock and Froelich, 1986; Murnane et al., 1989; Mortlock et al., 1993) are much higher than in normal seawater and other cool surface waters (Arnórsson, 1984). Therefore, Si-rich hydrothermal fluids circulating in Ge-rich rocks are able to leach more Ge than cold waters. The average Ge content of the siliceous rocks and siliceous limestones in Lincang are 78 and 67 ppm, i.e., 49 and 42 times higher, respectively, than those of UCC (Table 2). It is possible that the hydrothermal fluids may have carried and transported abundant Ge. Thus, the coal seams interbedded with hydrothermal sedimentary siliceous rocks in the Lincang region, should theoretically be more likely to enrich Ge (Hu et al., 1999).

Table 3
Oxygen and carbon isotopic compositions of the siliceous rocks and siliceous limestones from the Lincang germanium deposit.

Rock	Sample No.	$\delta^{18}O_{SMOW}$‰	Rock	Sample No.	$\delta^{13}C_{PDB}$‰	$\delta^{18}O_{SMOW}$‰
Siliceous rock	ZZ-19	13.9	Siliceous limestone	ZZ-58	6.1	18.0
	ZZ-27	13.8		ZZ-77	6.5	18.6
	ZZ-38	13.6		ZZ-84	6.9	18.7
	ZZ-45	10.9	Modern travertine	LMS-1	6.336	17.34
	ZZ-57	13.3		LMS-2	6.140	18.22
	ZZ-61	15.7		LMS-3	5.637	16.22
	ZZ-74	12.6	Spring water	LMS-4	5.928	16.95
	ZZ-79	14.3				
	ZZ-81	13.3				
	ZZ-87	13.5				
	ZZ-89	13.6				

Data of siliceous rock and limestone after Qi et al. (2002a, 2004).

5.4. Interaction between coal and Ge-bearing solutions

Many studies have shown Ge to be concentrated in the organic matter of coal rather than in admixed minerals. In particular, Ge is concentrated in the vitrain fraction and in lignite. These are materials generally thought to be derived from the woody parts of plants (Bernstein, 1985). Germanium is adsorbed by humic acids in peat and then forms stable complexes with lignin-derivative compounds containing orthodiphenol and orthohydroxyquinoid groups (Manskaya et al., 1972). Pokrovski and Schott (1998a,b) found that Ge forms complexes of the chelate type with the following functional groups: (1) carboxylic in acid solutions ($1 \le pH \le 6$), (2) di-phenolic hydroxyls in neutral and basic solutions ($pH \ge 6$), and (3) alcohol hydroxyls in very basic solutions ($pH \ge 10$). Weak alkaline ($pH = 10$) conditions contribute to the sorption of Ge by purified humic acids, and the quantity of complexed Ge is positively correlated with the initial Ge content of solutions at $pH = 10$ (Zhang et al., 1987). Increase of temperature not only enhances the solubility of Ge in hydrothermal solutions, but also increases the quantity of Ge complexed by organic matter in coal. Under acid conditions (initial $pH = 2.96$), at a given initial Ge content (5 mg/L) and 25–100 °C, the quantity of Ge complexed by peat and lignite was positively correlated with temperatures (Qi et al., 2005).

Vitrain is one of the least sorptive fractions of coal, indicating that Ge concentration must occur during the peat or lignite stages of coal formation, before vitrain forms (Bernstein, 1985). Ratynskiy et al. (1966) showed that hard coals, containing large amounts of vitrain, indeed absorbed far less Ge from aqueous solutions than did lignites. Based on laboratory experiments, they further deduced that, if Ge was sorbed from percolating aqueous solutions by already-formed coal, it would accumulate in those compounds concentrated in the heavy fractions (specific gravity >1.5) of coal matter. Actually, the reverse phenomenon occurs in Ge-bearing lignites or hard coals. For example, about 70% of total Ge in the mineralized lignites from the Lincang Ge deposit is concentrated in the light fractions (specific gravity <1.48) (Zhuang et al., 1998b). One may hence conclude that the accumulation of Ge from aqueous solutions after formation and burial of coal at great depths cannot be regarded as the main mode of entry of Ge into coal (Ratynskiy et al., 1966). Furthermore, the existence of fossil plant

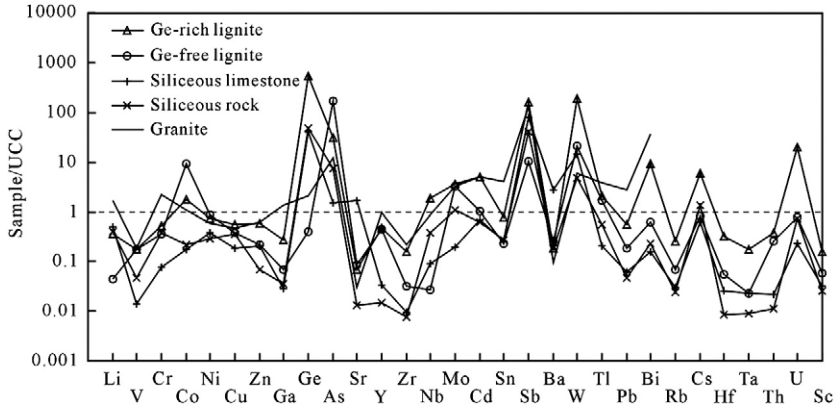

Fig. 10. Upper Continental Crust (UCC)-normalized mean trace element compositions of different rocks from the Lincang deposit. Different sample units show common enrichment of As, Sb, and W.

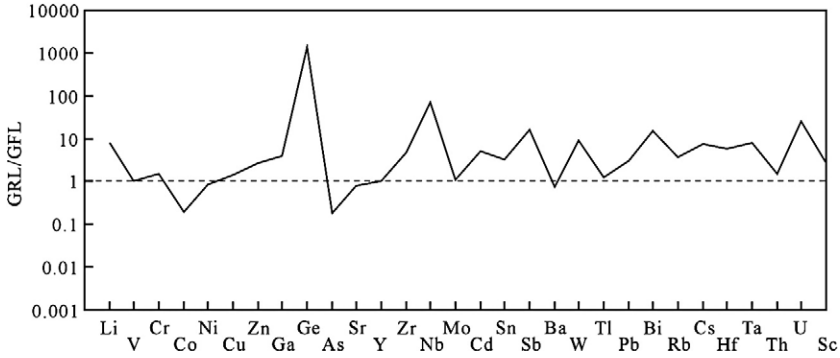

Fig. 11. Mean Ge-free lignite (GFL)-normalized trace element pattern of the Ge-rich lignite (GRL) from the Lincang deposit. Ge-rich lignite is enriched in most of the trace elements, particularly Ge, Nb, Li, Sb, W, Bi, and U, and depleted in Co and As, relative to Ge-free lignite.

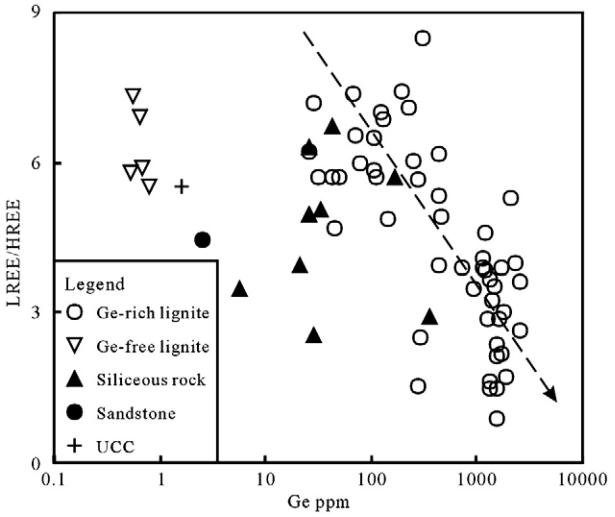

Fig. 12. Scatter diagram of LREE/HREE ratio *vs.* Ge content of different samples from the Lincang deposit. There is a distinct negative correlation between Ge content and LREE/HREE ratios of Ge-rich lignite. The most enriched Ge lignite and siliceous rocks show common low LREE/HREE ratios, indicating that enrichment of Ge and fractionation of REE occurred at the same time. UCC — Upper Continental Crust.

fragments in the siliceous rocks, as well as simultaneous enrichment of Ge and HREE in Ge-rich lignites, indicate that Ge in lignite from the Lincang deposit was mainly enriched during diagenesis.

5.5. Lincang granitic batholith as source of Ge

The Lincang granitic batholith that forms the basement of the Bangmai basin contains Ge concentrations ranging from 2.7 to 5.0 ppm with an average of 3.9 ppm (Hu et al., 1996). Normal granites contain 1.4 ppm (Taylor and McLennan, 1985). Thus the Lincang granites have about three times as much Ge as the average value for equivalent rocks. The Lincang granitic batholith thus has the potential to act as a source of Ge for the Lincang deposit.

Table 4
Sulfur isotopic compositions of sulfides from the Lincang germanium deposit.

Sample location	Mineral	Mineral occurrence	$\delta^{34}S$ ‰
Lengshuijing, Bangmai basin	Pyrite	Disseminated in lignite of N^4_{1b}	18.6
Ankeng, Bangmai basin	Pyrite	Disseminated in lignite of N^4_{1b}	28.6
Zhongzhai, Bangmai basin	Pyrite	Disseminated in lignite of N^2_{1b}	51.4
Zhongzhai, Bangmai basin	Pyrite	Disseminated in lignite of N^2_{1b}	40.4
Dazhai, Bangmai basin	Pyrite	Disseminated in lignite of N^2_{1b}	48.1
Dazhai, Bangmai basin	Pyrite	Disseminated in lignite of N^2_{1b}	41.4
Dazhai, Bangmai basin	Pyrite	Disseminated in lignite of N^2_{1b}	35.2
Dazhai, Bangmai basin	Pyrite	Disseminated in lignite of N^2_{1b}	21.7
Dazhai, Bangmai basin	Pyrite	Thin vein in lignite of N^2_{1b}	1.9
Dazhai, Bangmai basin	Pyrite	Thin vein in lignite of N^2_{1b}	0.2
Dazhai, Bangmai basin	Pyrite	Thin vein in lignite of N^2_{1b}	−5.4
Dazhai, Bangmai basin	Pyrite	Thin vein in lignite of N^2_{1b}	−3.4
Dazhai, Bangmai basin	Pyrite	Thin vein in lignite of N^2_{1b}	−1.0
Dazhai, Bangmai basin	Pyrite	Thin vein in lignite of N^2_{1b}	−0.8
Dazhai, Bangmai basin	Pyrite	Thin vein in lignite of N^2_{1b}	−5.1
Dazhai, Bangmai basin	Pyrite	Thin vein in lignite of N^2_{1b}	−2.6
Periphery of the Bangmai basin	Pyrite	Disseminated in quartz vein in granite	−0.6
Periphery of the Bangmai basin	Sphalerite	Disseminated in quartz vein in granite	−2.1
Periphery of the Bangmai basin	Sphalerite	Disseminated in quartz vein in granite	−3.8
Periphery of the Bangmai basin	Chalcocite	Disseminated in quartz vein in granite	−1.8
Periphery of the Bangmai basin	Chalcocite	Disseminated in quartz vein in granite	−2.0
Periphery of the Bangmai basin	Chalcocite	Disseminated in quartz vein in granite	−1.8
Periphery of the Bangmai basin	Chalcocite	Disseminated in quartz vein in granite	1.5
Periphery of the Bangmai basin	Galena	Disseminated in quartz vein in granite	−3.6

Data after Hu et al. (1996) and Zhang et al. (1996).

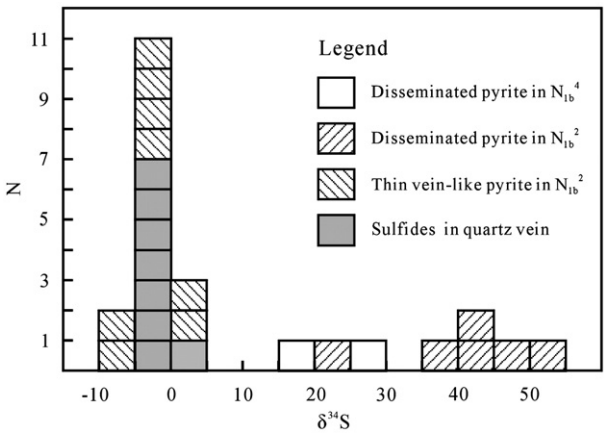

Fig. 13. Histogram of sulfur isotope data for sulfides from the Lincang deposit. Data after Hu et al. (1996) and Zhang et al. (1996). The sulfur isotopic compositions of pyrite in Ge-rich lignite from the basal coal-bearing unit indicate two different sulfur sources: sedimentary origin and granite-related materials.

Similar trace element patterns of different samples, including Ge-rich lignites, Ge-free lignites, siliceous rocks and siliceous limestones from the Lincang deposit, and from the basement granites, especially the common enrichment of As, Sb, and W (Table 2, Fig. 10), indicate that the granites may have been the source for most trace elements. This is also evidenced by the similarity in the REE patterns between Ge-rich lignites with Ge content <200 ppm, Ge-free lignites and underlying basement granites (Qi et al., 2004), as well as the similarity in sulfur isotope compositions of pyrite in Ge-rich lignites and those of sulfides in granite-related quartz veins (Table 4, Fig. 13).

Compared with REE compositions of granites, those of Ge-rich lignites with >200 ppm Ge, hydrothermal siliceous rocks and limestones show distinct enrichment of HREE. These differences may be attributed to REE fractionation during water-rock interactions, which occurred during the coal-forming or Si- and Ca-deposition processes. The final distribution of dissolved REE in the water-rock system is controlled by REE partitioning between calcite (or humic matter) and solution. For example, the experimental log K_d (REE) (REE partition coefficients between calcite and solution) show a convex tetrad effect variation (Tanaka et al., 2004), indicating that the deposition of Ca may result in the heterogenetic distribution of REE between calcite and solutions. Conditional binding constants for REE-HS (humic substances) interaction (K_c) increase from La to Lu by 2–3 orders of magnitude as a function of decreasing ionic radius (Sonke and Salters, 2006) or the log K pattern displays a MREE downward concavity (Pourret et al., 2007), indicating that humus in coal may preferentially complex with HREE or LREE.

6. An integrated model for the formation of the Lincang Ge deposit

We propose a new model involving formation of Ge-rich hydrothermal fluids, and transportation and deposition of Ge in coal seams.

6.1. Evidence for Ge-bearing hydrothermal fluids

As a result of Indian–Asian continent collision during the Himalayan orogeny, NW and EW-trending faults developed in the Lincang granitic batholith. These faults controlled not only the formation of the Bangmai basin but also Ge mineralization. Meteoric waters possibly penetrated downwards along faults and were heated by regional tectonism with an elevated geothermal gradient. The existence of the latter is supported by the occurrence of several modern hot springs of meteoric origin along fault systems in the district. The faults in the batholith acted as pathways for the heated

fluids. While moving, the hydrothermal fluids leached Ge, Si, Ca and other elements (Sb, W and U etc.) from the batholith. Seredin et al. (2006) noticed that alkaline N_2 or CO_2-rich hot (34.5–96.1 °C) spring waters exhibit anomalous higher concentrations of Ge, W, Mo, U, Sb and Be, compared to their average contents in river- and groundwaters. Concentrations of Mo and U in alkaline ground waters from Iceland are also observed to increase with increasing temperature and increasing age of these waters (Arnórsson and Óskarsson, 2007). The average Ge content of the siliceous rocks and siliceous limestones are, as stated above, 49 and 42 times higher, respectively, than those of UCC (Table 2). We believe that the hydrothermal fluids, which finally formed the inter-bedded siliceous rocks and limestones in the basal coal-bearing unit, may have carried and transported abundant Ge.

6.2. Transportation and deposition of Ge in coal seams

We deduce that the sites of the fault intersections are most probably the access channels of Ge-bearing hydrothermal fluids based on the following facts: (1) Ge-orebodies are controlled by contemporaneous faults which developed during deposition of the basal coal-bearing unit (N_{1b}^2); (2) Ge-orebodies are usually situated at the fault intersections in the basal coal-bearing unit (N_{1b}^2); and (3) Ge is concentrated at the top and bottom of coal seams where they are in contact with siliceous rocks and limestones. When the ascending hydrothermal solutions reached and interacted with the basal coal seams, Ge was scavenged from solution and complexed with humus in coal. With decrease in temperature, silica and calcium in solutions would be oversaturated and formed the interlayered siliceous rocks and siliceous limestones, which will be buried by future seams at the water-sediment interface. Interaction between coals and the Ge-bearing hydrothermal fluids during diagenesis may have then resulted in enrichment of Ge in the coal seams close to the fault intersections, and thus formation of the Lincang Ge deposit.

7. Summary and conclusions

(1) Layered siliceous rocks and siliceous limestones with hydrothermal textures and plant fragment fossils from the Lincang Ge deposit are characterized by low Al/(Al + Fe + Mn) (0.01 on average), and high U/Th ratios (>1). Their trace element, oxygen and/or carbon isotopic compositions are similar to those of hydrothermal sediments (chert, thermal springs, hot-spring siliceous sinter or hydrothermal travertine), indicating that these layered siliceous rocks and siliceous limestones are hydrothermal in origin. High Ge contents in these hydrothermal sedimentary rocks (78 and 67 ppm on average, respectively) imply that the hydrothermal solutions which formed the siliceous rocks and siliceous limestones, transported abundant Ge.

(2) Ge-rich lignites are distinctly enriched in Ge, Nb, Li, Sb, W, Bi, and U, and depleted in As and Co, compared with Ge-free lignites. When normalized to NASC or Ge-free lignites, REE patterns of Ge-rich lignites show distinct enrichment of HREE with the increase in Ge contents in these lignites. Sulfides in Ge-rich lignites can be divided into two groups with different sulfur isotopic composition, disseminated pyrites ($\delta^{34}S$ values vary from 17.2‰ to 51.4‰, similar to those of pyrites in Ge-free lignites) and thin vein-like (or gel like) pyrites ($\delta^{34}S$ values range from 1.9‰ to −5.4‰, similar to those of the sulfides in granite-related quartz veins).

(3) Germanium ore-bodies have equant or elongated configurations and are mainly distributed at fault intersections. Germanium appears to be concentrated at the top and bottom of coal seams, and where they are mainly in contact with siliceous rocks or siliceous limestones. With increasing Ge contents, LREE/HREE ratios and REE patterns of Ge-rich coals are much alike those of the siliceous rocks. It is concluded that circulating hydrothermal fluids extracted Ge from the granitic batholiths. The fluids were discharged into the basin along faults. Precipitation of Ge took place along with Si and Ca, which formed Ge-rich siliceous rocks and siliceous limestones. Ge was also complexed or absorbed by organic matters of coal seams in the basal coal-bearing unit to form the Lincang Ge deposit.

Acknowledgements

This research was supported jointly by the Knowledge-innovation Program of the Chinese Academy of Sciences (KZCX2-YW-111), the National 973 Program of China (2007CB411408) and the National Natural Science Foundation of China (40302018, 49925309). The authors appreciate Frank Melcher for the constructive suggestions and comments in his review of the manuscript.

References

Adachi, M., Yamamoto, K., Suigiaki, R., 1986. Hydrothermal chert and associated siliceous rocks form the northern Pacific: their geological significance as indication of ocean ridge activity. Sedimentary Geology 47, 125–148.
Arnórsson, S., 1984. Germanium in Icelandic geochermal systems. Geochemica et Cosmochemica Acta 48, 2489–2502.
Arnórsson, S., Óskarsson, N., 2007. Molybdenum and tungsten in volcanic rocks and in surface and <100 °C ground waters in Iceland. Geochimica et Cosmochimica Acta 71, 284–304.
Bernstein, L.R., 1985. Germanium geochemistry and mineralogy. Geochemica et Cosmochemica Acta 49, 2409–2422.
Boström, K., Rydell, H., Joensuu, O., 1979. Långban: an exhalative sedimentary deposit? Economic Geology 74, 1002–1011.
Breger, I.A., Schopf, J.M., 1955. Germanium and uranium in coalified wood from upper Devonian black shale. Geochimica et Cosmochimica Acta 7, 287–293.
Chen, D.Z., Wang, J.G., Qing, H.R., Yan, D.T., Li, R.W., 2009. Hydrothermal venting activities in the Early Cambrian, South China: petrological, geochronological and stable isotopic constraints. Chemical Geology 258, 168–181.
Chen, R.Q., Long, B., Cao, C.C., 1996. Rare earth element distribution patterns of coals in Guangxi. Guangxi Sciences 3 (2), 32–36 (in Chinese).
Chen, X.P., Chen, D.F., 1990. Geochemistry of Upper Devonian hydrothermal mammilated chert in Guangxi, Southwest China. Chinese Journal of Geochemistry 9 (1), 46–53 (in Chinese with English abstract).
Clayton, R.N., 1986. High temperature isotope effects in the early solar system. Reviews in Mineralogy and Geochemistry 16, 129–140.
Crerar, D.A., Namson, J., Chyi, M.S., Williams, L., Feigenson, M.D., 1982. Manganiferous chert of the Franciscan assemblage: general geology ancient and modern analogues and implications for hydrothermal convection at oceanic spreading centers. Economic Geology 77, 519–540.
Eškenazy, G., 1996. Factors controlling the accumulation of trace elements in coal, Annuaire de 1'Universite de Sofia St. Kliment Ohridski, Faculte de Geologie et Geographie, Livre 1. Geologie 89, 219–236.
Finkelman, R.B., 1982. Modes of occurrence of trace elements and minerals in coal: an analytical approach. In: Filby, R.H. (Ed.), Atomic and Nuclear Methods in Fossil Energy Research. Plenum, New York, pp. 141–149.
Goldschmidt, V.M., Peters, C., 1933. Über die Anreicherung seltener Elemente in Steinkohlen. Nachrichten von der Gesellschaft der Wissenschaften zu Göttingen, Mathematisch-Physischen Klasse IV, 371–387.
Guberman, D.E., 2008. Germanium [Advance Release]. U.S. Geological Survey Minerals Yearbook, pp. 30.1–30.5. 2007.
Guberman, D.E., 2009. Germanium. U.S. Geological Survey. Mineral Commodity Summaries, January 2009, 2 pp. http://minerals.usgs.gov/minerals/pubs/commodity/germanium/index.html#mcs.
Hallam, A., Payne, K.W., 1958. Germanium enrichment in lignites from the lower Lias of Dorset. Nature 181, 1008–1009.
Han, Y.R., Yuan, Q.B., Li, Y.H., Zhang, L., Dai, J.M., 1994. Dazhai superlarge uranium-bearing germanium deposit in Western Yunnan Region: metallogenic geological conditions and prospect. China Nuclear Science & Technology Report. Nuclear Energy Press, Beijing, pp. 3–12 (in Chinese with English abstract).
Höll, R., Kling, M., Schroll, E., 2007. Metallogenesis of germanium — a review. Ore Geology Reviews 30, 145–180.
Hou, Z., Cook, N.J., 2009. Metallogenesis of the Tibetan collisional orogen: A review and introduction to the special issue. Ore Geology Reviews 36, 2–24 (this issue).
Hower, J.C., Ruppert, L.F., Williams, D.A., 2002. Controls on boron and germanium distribution in the low-sulfur Amos coal bed, Western Kentucky coalfield, USA. International Journal of Coal Geology 53, 27–42.
Hu, R.Z., Bi, X.W., Su, W.C., Qi, H.W., 1999. Ge-rich hydrothermal solution and abnormal enrichment of Ge in coal. Chinese Science Bulletin 44 (suppl. 2), 257–258.
Hu, R.Z., Bi, X.W., Ye, Z.J., Su, W.C., 1996. The genesis of Lincang germanium deposit: a preliminary investigation. Chinese Journal of Geochemistry 15, 44–50.
Krejci-Graf, K., 1983. Minor elements in coal. In: Augustithis, S.S. (Ed.), The Significance of Trace Elements in Solving Petrogenic Problems and Controversies. Theophrastus Publishers, Athens, pp. 553–597.

Kulinenko, O.R., 1977. Relationship between germanium content and seam thickness in Paleozoic paralic coal basins of Ukraine. International Geology Review 19, 1178–1182.
Kunzendorf, H., Stoffers, P., Gwozdz, R., 1988. Regional variations of REE patterns in sediments from active plate boundaries. Marine Geology 84, 191–199.
Lewis, B.L., Froelich, P.N., Andreae, M.O., 1985. Methyl germanium in natural waters. Nature 313, 303–305.
Li, X.L., 1996. Basic characteristics and formation structural environment of Lincang composite granite batholith. Yunnan Geology 15, 1–18 (in Chinese with English abstract).
Li, Y.H., 2000. The geological characteristics of Lincang Ge deposit. Yunnan Geology 19, 263–269 (in Chinese with English abstract).
Liu, J.J., Zhen, M.H., Liu, J.M., Zhou, Y.F., Gu, X.X., Zhang, B., 1999. The geological and geochemical characteristics of Cambrian chert and their sedimentary environmental implication in western Qinling. Acta Petrologica Sinica 15, 145–154 (in Chinese with English abstract).
Ma, L.F., 2002. Geological Atlas of China. Geological Press, Beijing. 348 pp. (in Chinese).
Manskaya, S.M., Kodina, V.N., Generalova, V.N., Kravtsova, R.P., 1972. Interaction between germanium and lignin structure in the early stages of formation of coal. Geokhimiya 5, 600–609.
Marchig, V., Gundlach, H., Möller, P., Schley, F., 1982. Some geological indicators for discrimination between diagenetic and hydrothermal matalliferous sediments. Marine Geology 50, 241–256.
Middlesworth, P.E., Wood, S.A., 1998. The aqueous geochemistry of the rare earth elements and yttrium. Part 7. REE, Th and U contents in the thermal springs associated with the Idaho batholith. Applied Geochemistry 13, 861–884.
Minčev, D., Eškenazi, G., 1963. Germanium in den Gagatkohlen des Bezirks Pleven. Comptes Rendus de 1'Académie Bulgare des Sciences 16, 537–540.
Mo, X.X., Lu, F.X., Shen, S.Y., Zhu, Q.W., Hou, Z.Q., Yang, K.H., Deng, J.F., Liu, X.P., He, C.X., 1993. Volcanism and mineralization in Sanjiang region, Southwest China. Geological Press, Beijing. 197 pp. (in Chinese).
Mortlock, R.A., Froelich, P.N., 1986. Hydrothermal germanium over the Southern East Pacific Rise. Science 231, 43–45.
Mortlock, R.A., Froelich, P.N., Feely, R.A., Massoth, G.J., Butterfield, D.A., Lupton, J.E., 1993. Silica and germanium in Pacific Ocean hydrothermal vents and plums. Earth and Planetary Science Letters 119, 365–378.
Murnane, R.J., Leslie, B.L., Hammond, D.E., 1989. Germanium geochemistry in the Southern California Borderlands. Geochemica et Cosmochimica Acta 53, 2873–2882.
Murray, R.W., Brink, M.R., Jones, D.L., Geriach, D.C., Russ, G.P., 1990. Rare earth elements as indicators of different marine depositional environments in chert and shale. Geology 18, 268–271.
Pokrovski, G.S., Schott, J.A., 1998a. Thermodynamic properties of aqueous Ge(IV) hydroxide complexes from 25 to 350 °C: Implications for the behavior of Ge and the Ge/Si ratio in hydrothermal fluids. Geochimica et Cosmochimica Acta 62, 1631–1642.
Pokrovski, G.S., Schott, J.A., 1998b. Experimental study of the complexation of silicon and germanium with aqueous organic species: implications for germanium and silicon transport and Ge/Si ratio in natural waters. Geochimica et Cosmochimica Acta 62, 3413–3428.
Pourret, O., Davranche, M., Gruau, G., Dia, A., 2007. Rare earth elements complexation with humic acid. Chemical Geology 243, 128–141.
Qi, H.W., Hu, R.Z., Su, W.C., Qi, L., 2002a. Genesis of carboniferous siliceous limestone in the Lincang germanium deposit and its relation with germanium mineralization. Geochimica 31, 161–168 (in Chinese with English abstract).
Qi, H.W., Hu, R.Z., Su, W.C., Qi, L., 2002b. REE geochemistry of lignites in Lincang germanium deposit, Yunnan Province. Geochimica 31, 300–308 (in Chinese with English abstract).
Qi, H.W., Hu, R.Z., Su, W.C., Qi, L., Feng, J.Y., 2004. Continental hydrothermal sedimentary siliceous rock and genesis of superlarge germanium (Ge) deposit hosted in coal: a study from the Lincang Ge deposit, Yunnan, China. Sciences in China (Series D) 47, 973–984.
Qi, H.W., Hu, R.Z., Qi, L., 2005. Experimental study on the interaction between peat, lignite and germanium-bearing solution at low temperature. Sciences in China (Series D) 48, 1411–1417.
Qi, H., Hu, R., Zhang, Q., 2007. REE Geochemistry of the Cretaceous lignite from Wulantuga Germanium Deposit, Inner Mongolia, Northeastern China. International Journal of Coal Geology 71, 329–344.
Ratynskiy, V.M., Sendul'skaya, T.L., Shpirt, M.Y., 1966. Chief mode of entry of germanium into coal. Doklady Earth Science Sections 170, 218–221.
Rona, P.A., 1984. Hydrothermal mineralization at seafloor spreading centers. Earth Science Reviews 20, 1–104.
Seredin, V.V., 2003. Anomalous trace elements contents in the Spetsugli germanium deposit (Pavlovka brown coal deposit) Southern Primorye: communication 1. antimony. Lithology and Mineral Resources 38, 154–161.
Seredin, V.V., 2005. Rare earth elements in germanium-bearing coal seams of the Spetsugli deposit (Primor'e region, Russia). Geology of Ore Deposits 47, 238–255.
Seredin, V.V., Danilcheva, J., 2001. Coal-hosted Ge deposits of the Russian Far East. In: Piestrynsky, A., et al. (Ed.), Mineral Deposits at the Beginning of the 21st Century. Swets & Zeitlinger Publishers, Lisse, pp. 89–92.
Seredin, V.V., Danilcheva, Y.A., Magazina, L.O., Sharova, I.G., 2006. Ge-bearing coals of the Luzanovka Graben, Pavlovka Brown Coal Deposit, Southern Primorye. Lithology and Mineral Resources 41, 280–301.
Smirnov, V.I., 1977. Ore deposits of the USSR, vol. I and II. Pitman Publishing, London. 1286 pp.
Sonke, J.E., Salters, V.J.M., 2006. Lanthanide-humic substances complexation. I. Experimental evidence for a lanthanide contraction effect. Geochimica et Cosmochimica Acta 70, 1495–1506.
Sun, C.X., 2002. The origin and REE geochemistry of the red clay weathering crusts in karst regions of Guizhou Province. Unpublished Dissertation, Institute of Geochemistry, Chinese Academy of Sciences, unpublished, 81 pp.
Taylor, S.R., McLennan, S.M., 1985. The continental crust: Its composition and evolution. Blackwell Scientific Publications, Oxford. 312 pp.
Tanaka, K., Ohta, A., Kawabe, I., 2004. Experimental REE partitioning between calcite and aqueous solution at 25 °C and 1 atm: constraints on the incorporation of seawater REE into seamount-type limestones. Geochemical Journal 38, 19–32.
Tu, G.Z., 1988. Geochemistry of the strata-bound mineral deposits of China. Science Press, Beijing. 388 pp. (in Chinese).
Vassilev, S.V., Eskenazy, G.M., Tarassov, M.P., Dimov, V.I., 1996. Mineralogy and geochemistry of a vitrain lens with unique trace element content from the Vulche Pole coal deposit, Bulgaria. Geologica Balcanica 25, 111–124.
Wang, J.H., Yan, W., Chang, X.Y., Xie, G.H., Qiu, H.N., Dong, J.Q., Zhang, L.Y., 1998. Continental hydrothermal sedimentation: a case study of the Yunnan area, China. Geological Publishing House, Beijing, pp. 23–31 (in Chinese with English abstract).
Weber, J.N. (Ed.), 1973. Geochemistry of Germanium. Dowden. Hutchinson & Ross, Inc., Stroudsburg, Pennsylvania. 466 pp.
Wu, H.O., Chen, R.Q., Lin, G., 1994. Geochemistry of rare earth element in coals. Journal of Guilin College of Geology 14 (3), 284–294 (in Chinese with English abstract).
Yamamoto, K., 1987. Geochemical characteristics and depositional environments of cherts and associated rocks in the Franciscan and Shimanto terranes. Sedimentary Geology 52, 65–108.
Yao, L.B., Gao, Z.M., Yang, Z.S., Long, H.B., 2002. Origin of seleniferous cherts in Yutangba Se deposit, southwest Enshi, Hubei Province, China. Science in China (series D) 45, 741–754.
Yudovich, Y.E., 2003. Notes on the marginal enrichment of germanium in coal beds. International Journal of Coal Geology 56, 223–232.
Zhang, L., Han, Y.R., Yuan, Q.B., 1996. Germanium sources and geological characteristics of Ge orefield in Lincang, Yunnan. Unpublished internal report, No. 209 Geological Team, Southwest Bureau of Geologic Exploration. China National Nuclear Corporation, pp. 3–15 (in Chinese).
Zhang, S.L., Yin, J.S., Wang, S.Y., 1987. Study on existent forms of germanium in coal, Bangmai Basin, Yunnan. Acta Sedimentologica Sinica 6, 29–41 (in Chinese with English abstract).
Zhong, D.L., 1998. Paleo-Tethys orogenic belt in Western Sichuan and Yunnan. Science Press, Beijing. 331 pp. (in Chinese).
Zhuang, H.P., Lu, J.L., Fu, J.M., Liu, J.Z., 1998a. Lincang superlarge germanium deposit in Yunnan Province, China: sedimentation, diagenesis, hydrothermal process and mineralization. Journal of China University of Geosciences 9, 129–136.
Zhuang, H.P., Lu, J.L., Fu, J.M., Liu, J.Z., Ren, C.G., Zou, D.G., 1998b. Germanium occurrence in Lincang superlarge deposit in Yunnan, China. Science in China (series D) 41 (supplement), 21–27.